

Synthesis, Crystal Structures, and Third-Order Nonlinear Optical Properties of a Series of Ferrocenyl Organometallics

Gang Li,[†] Yinglin Song,[‡] Hongwei Hou,^{*†} Linke Li,[†] Yaoting Fan,[†] Yu Zhu,[†] Xiangru Meng,[†] and Liwei Mi[†]

Department of Chemistry, Zhengzhou University, Henan 450052, P.R. China, and Department of Applied Physics, Harbin Institute of Technology, Heilongjiang 150001, P.R. China

Received July 10, 2002

Three novel ferrocenyl complexes [Zn(4-PFA)₂(NO₃)₂](H₂O) (**1**), [Hg₂(OAc)₄(4-BPFA)₂](CH₃OH) (**2**), and [Cd₂(OAc)₄(4-BPFA)₂] (**3**) (4-PFA = [(4-pyridylamino)carbonyl]ferrocene, 4-BPFA = 1,1'-bis[(4-pyridylamino)carbonyl]ferrocene) were prepared, and complexes **1** and **2** were structurally characterized by means of X-ray single-crystal diffraction. In complex **1**, the zinc(II) atom is coordinated at a distorted tetrahedral environment by two nitrogen atoms from two 4-PFA moieties and two oxygen atoms from two nitrate anions; [Zn(4-PFA)₂(NO₃)₂] units are linked by hydrogen bonds N–H···O and O–H···O forming one-dimensional chains. Complex **2** is a tetranuclear macrocycle compound consisting of two 4-BPFA moieties and two Hg atoms; [Hg₂(OAc)₄(4-BPFA)₂] units form 1-D chains by hydrogen bonds N–H···O as complex **1**. Some complexes with 1,1'-bisubstituted pyridine-containing ferrocene ligands have been described, but their crystal data are limited. Compound **2** is the first example of a macrocyclic pyridine-containing ferrocenyl complex. The third-order nonlinear optical (NLO) properties of 4-PFA, 4-BPFA, and complexes **1–3** were determined by Z-scan techniques. The results indicate that all the compounds exhibit strong self-focusing effect. The hyperpolarizability γ values are calculated to be in the range 1.51×10^{-28} to 3.12×10^{-28} esu. The γ values are nearly twice as large for complexes **1–3** as for their individual ligands, showing that the optical nonlinearity of the complexes is dominated by the ligands.

Introduction

The attachment of mono- or polypyridyl fragments to a ferrocenyl group has attracted much attention due to their potential various applications: electrochemical sensors, potential antitumor agents, monomers for extended stacked complexes, and even units for self-assembly.¹ Up to now, a large number of pyridine-containing ferrocene derivatives and their related complexes have been described.² For example Sun and co-workers have reported the photophysical and photochemical properties of W(0) and Re(I) carbonyl

complexes incorporating ferrocenyl-substituted pyridine ligands.^{2a} Moutet and co-workers have studied the electrochemical properties of ferrocenyl complexes bearing terpyridine or phenanthroline ligands.^{2b} Fang et al. have also

* Author to whom correspondence should be addressed. E-mail: houghongw@zzu.edu.cn. Phone and fax: +86-371-7761744.

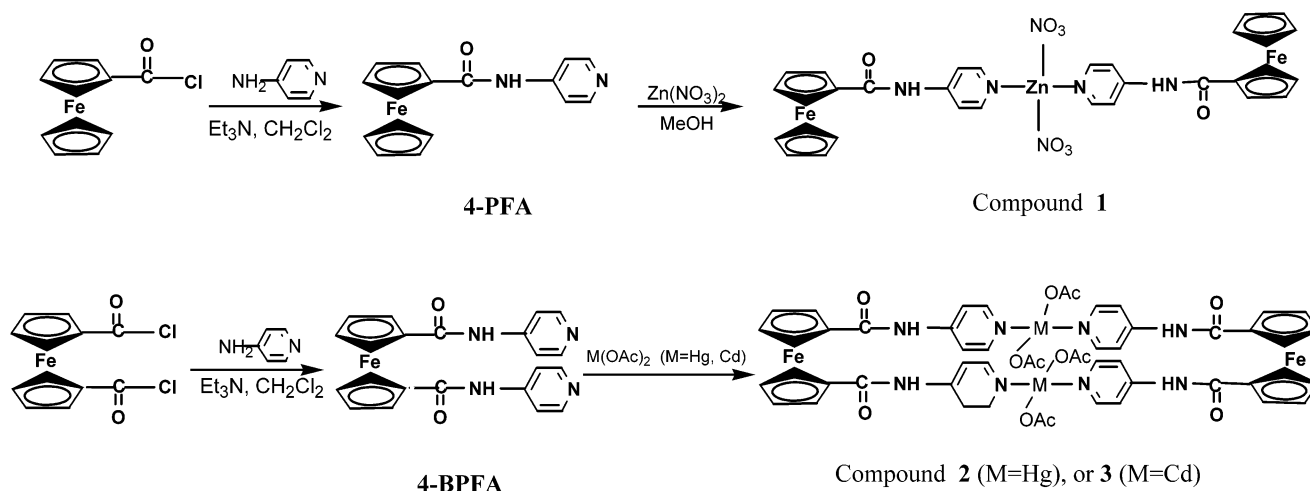
[†] Zhengzhou University.

[‡] Harbin Institute of Technology.

(1) (a) Togni, A.; Hayashi, T. *Ferrocenes. Homogeneous Catalysis, Organic Synthesis, Materials Science*; VCH: Weinheim, 1995. (b) Butler, L. R. *Polyhedron* **1992**, *11*, 3117. (c) Long, N. J. *Metalloenes*; Blackwell: Oxford, 1998. (d) Beer, P. D.; Gale, P. A.; Chen, G. Z. *J. Chem. Soc., Dalton Trans.* **1999**, 1897. (e) Valério, C.; Fillaut, J. L.; Ruiz, J.; Guittard, J.; Blais, J. C. and Astruc, D. *J. Am. Chem. Soc.* **1997**, *119*, 2588. (f) Carr, J. D.; Coles, S. J.; Hassan, W. W.; Hursthouse, M. B.; Malik, K. M. A.; Tucker, H. R. *J. Chem. Soc., Dalton Trans.* **1999**, 57.

(2) (a) Sun, S. S.; Tran, D. T.; Odongo, O. S.; Lees, A. J. *Inorg. Chem.* **2002**, *41*, 132. (b) Moutet, J. C.; Eric, S. A.; Royal, G.; Tingry, S.; Ziessel, R. *Eur. J. Inorg. Chem.* **2002**, 692. (c) Fang, C. J.; Duan, C. Y.; He, C.; Meng, Q. J.; Liu, Y. J.; Mei, Y. H.; Wang, Z. M. *Organometallics* **2001**, *20*, 2525. (d) Barranco, E. M.; Crespo, O.; Gimeno, M. C.; Jones, P. G.; Laguna, A.; Sarroca, C. *J. Chem. Soc., Dalton Trans.* **2001**, 2523. (e) Sprigings, T. G.; Hall, C. D. *Organometallics* **2001**, *20*, 2560. (f) Constable, E. C.; Edwards, A. J.; Marcos, M. D.; Raithby, P. R.; Máñez, R. M.; Tendero, M. J. L. *Inorg. Chim. Acta* **1994**, *224*, 11. (g) Mata, J. A.; Uriel, S.; Llusar, R.; Peris, E. *Organometallics* **2000**, *19*, 3797. (h) Moriuchi, T.; Yoshida, K.; Hirao, T. *Organometallics* **2001**, *20*, 3101. (i) Carr, J. D.; Coles, S. J.; Hursthouse, M. B.; Light, M. E.; Munro, E. L.; Tucker, J. H. R.; Westwood, J. *Organometallics* **2000**, *19*, 3312. (j) Fang, C. J.; Duan, C. Y.; Guo, D.; He, C.; Meng, Q. J.; Wang, Z. M.; Yan, C. H. *Chem. Commun.* **2001**, 2540. (k) Xue, W. M.; Kühn, F. E.; Herdtweck, E.; Li, Q. *Eur. J. Inorg. Chem.* **2001**, 213. (l) Bhadbhade, M. M.; Das, A.; Jeffery, J. C.; McCleverty, J. A.; Badiola, J. A. N. B.; Ward, M. D. *J. Chem. Soc., Dalton Trans.* **1995**, 2769. (m) Wong, W. Y.; Wong, W. T.; Cheung, K. K. *J. Chem. Soc., Dalton Trans.* **1995**, 1379. (n) Sakanishi, S.; Bardwell, D. A.; Couchman, S.; Jeffery, J. C.; McCleverty, J. A.; Ward, M. D. *J. Organomet. Chem.* **1997**, *528*, 35.

Scheme 1



described the structures and electrochemistry properties of several complexes $[\text{CuL}^1(\text{CH}_3\text{CN})][\text{ClO}_4]$, $[\text{AgL}^1(\text{CH}_3\text{CN})][\text{BF}_4]$, and $[\text{AgL}^1][\text{BF}_4]$ ($\text{L}^1 = [(\text{C}_5\text{H}_4\text{N})\text{CHNNC}(\text{CH}_3)(\text{C}_5\text{H}_4)]_2\text{Fe}$).^{2c}

On the other hand, ferrocene-containing molecules with nonlinear optical properties are currently attracting a great deal of attention.^{3,4} Compared to organic molecules, organometallic complexes have some definitive advantages such as tunability of the polarizability by changing the oxidation state of the metal atoms or by varying the ligands.⁴ Pyridine-containing ferrocenyl compounds have drawn much attention in this context. Several groups have studied the nonlinear optical (NLO) properties of some compounds,⁵ but they focused their attention on second-order NLO properties; investigations of third-order NLO properties are lacking.

It is well-known that third-order NLO materials can be used for a number of photonic applications, for example, optical signal processing, optical communication, optical computing, electro-optic modulation, optical limiting effect, and so forth.⁶ Thus, design and synthesis of new molecules with large macroscopic optical nonlinearities represent an

active research field in modern chemistry and materials science. We are currently interested in searching for new potential third-order NLO materials. Pyridine-containing ferrocenyl complexes consist of two parts: ferrocenyl ligands and metal ions. Both of the two parts may make an important contribution to optical nonlinearity of ferrocenyl complexes. Herein, we synthesized ferrocenyl ligands [(4-pyridylamino)carbonyl]ferrocene (4-PFA) and 1,1'-bis[(4-pyridylamino)carbonyl]ferrocene (4-BPFA), and their corresponding complexes $[\text{Zn}(4\text{-PFA})_2(\text{NO}_3)_2](\text{H}_2\text{O})$ (**1**), $[\text{Hg}_2(\text{OAc})_4(4\text{-BPFA})_2](\text{CH}_3\text{OH})$ (**2**), and $[\text{Cd}_2(\text{OAc})_4(4\text{-BPFA})_2]$ (**3**) (See Scheme 1). The crystal structures of complexes **1** and **2** were characterized by X-ray diffraction. In compound **1**, the zinc(II) ion is in a distorted tetrahedral environment with two 4-PFA ligands and two nitrate anions. Compound **2** is a novel tetranuclear macrocycle complex with dimensions $4.312 \times 19.589 \text{ \AA}^2$. To our knowledge, **2** represents the first example of a macrocyclic pyridine-containing ferrocenyl complex. Moreover, all five compounds have strong third-order NLO refractive properties. The calculated hyperpolarizability γ values are in the range 1.51×10^{-28} to 3.12×10^{-28} esu. The results indicate that the NLO properties of the complexes are dominated by ligands 4-PFA or 4-BPFA, and the contribution of post-transition metals Zn, Cd, or Hg to optical nonlinearity is small.

Experimental Section

Materials and Physical Techniques. All chemicals were of reagent grade quality obtained from commercial sources and used without further purification. Chlorocarbonylferrocene⁷ and 1,1'-bis(chlorocarbonyl)ferrocene^{1f} were prepared according to literature procedures.

IR data were recorded on a Nicolet NEXUS 470-FTIR spectrophotometer with KBr pellets in the $400\text{--}4000 \text{ cm}^{-1}$ region. UV-vis spectra were obtained on an HP 8453 spectrophotometer. Elemental analyses (C, H, and N) were carried out on a Carlo-Erba 1106 elemental analyzer. ¹H NMR spectra were recorded at room temperature (RT) on Bruker DPX 400 spectrometers.

Preparation of [(4-Pyridylamino)carbonyl]ferrocene (4-PFA). The same method as that used for 4-BPFA⁸ was carried out, adding

(7) Lorkowski, H. J.; Pannier, R.; Wende, A. *J. Prakt. Chem.* **1967**, *35*, 149.

(3) (a) Davies, D. A.; Silver, J.; Cross, G.; Thomas, P. J. *J. Organomet. Chem.* **2001**, *631*, 59. (b) Jayaprakash, K. N.; Ray, P. C.; Matsuoka, I.; Bhadbhade, M. M.; Puranik, V. G.; Das, P. K.; Nishihara, H.; Sarkar, A. *Organometallics* **1999**, *18*, 3851. (c) Lee, I. S.; Seo, H.; Chung, Y. K. *Organometallics* **1999**, *18*, 1091. (d) Nguyen, P.; Gómez-Elipe, P.; Manners, I. *Chem. Rev.* **1999**, *99*, 1515. (e) Blanchard-Desce, Runser, M. C.; Fort, A.; Barzoukas, M.; Lehn, J. M.; Alain, V. *Chem. Phys.* **1995**, *199*, 253. (f) Marder, S. R.; Perry, J. W.; Schaefer, W. P. *Organometallics* **1986**, *10*, 191. (g) Green, M. L. H.; Marder, S. R.; Thompson, M. E.; Bandy, J. A.; Bloor, D.; Kolinsky, P. V.; Jones, R. J. *Nature* **1987**, *330*, 360.

(4) Long, N. J. *Angew. Chem., Int. Ed. Engl.* **1995**, *34*, 21.

(5) (a) Lin, J. T.; Sun, S. S.; Wu, J. J.; Liaw, Y. C.; Lin, K. J. *J. Organomet. Chem.* **1996**, *517*, 217. (b) Lin, J. T.; Sun, S. S.; Wu, J. R.; LiawLee, L.; Lin, K. J.; Huang, Y. F. *Inorg. Chem.* **1995**, *34*, 2323. (c) Yeung, L. K.; Kim, J. E.; Chung, Y. K.; Rieger, P. H.; Sweigart, D. A. *Organometallics* **1996**, *15*, 3891. (d) Briel, O.; Sünkel, K.; Krossing, I.; Nöth, H.; Schmälzlin, E.; Meerholz, K.; Bräuchle, C.; Beck, W. *Eur. J. Inorg. Chem.* **1999**, 483. (e) Mata, J.; Uriel, S.; Peris, E.; Llusar, R.; Houbrechts, S.; Persoons, A. *J. Organomet. Chem.* **1998**, *562*, 197. (f) Lee, I. S.; Chung, Y. K.; Mun, J.; Yoon, C. S. *Organometallics* **1998**, *18*, 5080. (g) Lee, I. S.; Lee, S. S.; Chung, Y. K.; Kim, D.; Song, N. W. *Inorg. Chim. Acta* **1998**, *279*, 243.

(6) (a) Martellucci, S.; Chester, A. N. *Nonlinear optics and Optical Computing*; Plenum Press: New York, 1990. (b) Karna, S. P.; Yeates, A. T. *Nonlinear Optical Material*; American Chemical Society: Washington, DC, 1996.

chlorocarbonylferrocene (2.236 g, 9.0 mmol) in anhydrous CH₂-Cl₂ (120 mL) to a stirred mixture of 4-aminopyridine (0.847 g, 9.0 mmol), 4-(dimethylamino)pyridine (0.0274 g, 0.23 mmol), and triethylamine (3.25 mL, 22.5 mmol) in anhydrous CH₂Cl₂ (30 mL) under nitrogen at 0 °C. The reaction mixture was stirred at 0 °C for 7 h and at room temperature for 15 h. Saturated NaHCO₃ aqueous solution (40 mL) was then added, and the mixture was extracted with CH₂Cl₂ (3 × 30 mL). The combined extracts were dried over MgSO₄ and filtered, and the solvent was removed under reduced pressure to give an orange solid. The compound may be recrystallized from CHCl₃ to give orange needles; yield, 76%. IR (cm⁻¹): 3240 (NH), 1671 (C=O), 1589 (C=C), 499 (Fe–Cp). Anal. Calcd for C₁₆H₁₄ON₂Fe: C, 62.77; H, 4.61; N, 9.15%. Found: C, 62.61; H, 4.58; N, 8.94%. ¹H NMR (400 MHz, CDCl₃): δ 8.52 (s, 1H, NH), 7.80 (m, 2H, C₅H₄N), 7.62 (s, 2H, C₅H₄N), 4.87 (s, 2H, C₅H₄), 4.47 (s, 2H, C₅H₄), 4.25 (s, 5H, C₅H₅).

Preparation of 1,1'-Bis[(4-pyridylamino)carbonyl]ferrocene (4-BPFA). 4-BPFA was prepared according to the literature.⁸ Elemental analysis and IR and ¹H NMR spectra were consistent with those previously reported.

Preparation of [Zn(4-PFA)₂(NO₃)₂](H₂O) (1). A solution of 4-PFA (0.0612 g, 0.2 mmol) in methanol (5 mL) was added dropwise to a solution of Zn(NO₃)₂·6H₂O (0.0297 g, 0.10 mmol) in methanol (7 mL). The resulting solution was allowed to stand at room temperature in the dark. Red crystals suitable for X-ray single crystals analysis were obtained over 24 h in 58% yield, mp 168–169 °C. IR (cm⁻¹): 3316 (NH), 1655 (C=O), 1592 (C=C), 1384 (N–O), 498 (Fe–Cp). Anal. Calcd for C₅₁H₅₈AgFe₄N₅O₅: C, 46.85; H, 3.66; N, 10.25%. Found: C, 47.03; H, 3.68; N, 9.90%. ¹H NMR (400 MHz, DMSO): δ 9.75 (m, 2H, NH), 8.44 (s, 4H, C₅H₄N), 7.77 (s, 4H, C₅H₄N), 5.05 (s, 4H, C₅H₄), 4.52 (s, 4H, C₅H₄), 4.23 (s, 10H, C₅H₅).

Preparation of [Hg₂(OAc)₄(4-BPFA)₂](CH₃OH) (2). To a solution of Hg(OAc)₂ (0.0160 g; 0.05 mmol) in methanol (6 mL) was slowly added 4-BPFA (0.0213 g, 0.05 mmol) in ethanol (6 mL) at room temperature. After the resulting mixture stood in the dark for 2 days, dark-red crystals of **2** suitable for X-ray structure determination were formed in 64% yield. IR (cm⁻¹): 3386 (NH), 1686 (C=O), 1596 (C=C), 498 (Fe–Cp). Anal. Calcd for C₅₄H₅₆N₈O₁₄Fe₂Hg₂: C, 41.74; H, 3.63; N, 7.21%. Found: C, 41.55; H, 3.78; N, 6.94%. ¹H NMR (400 MHz, DMSO): δ 9.76 (m, 4H, NH), 8.35 (s, 8H, C₅H₄N), 7.62 (s, 8H, C₅H₄N), 5.07 (s, 8H, C₅H₄), 4.55 (s, 8H, C₅H₄), 1.91 (s, 12H, CH₃COO).

Preparation of [Cd₂(OAc)₄(4-BPFA)₂] (3). Complex **3** was prepared in a manner analogous to that used to prepare complex **2**. Reaction of Cd(OAc)₂·2H₂O with 4-BPFA gave **3** as red single crystals. Crystals of **3** are stable in the air. Yield: 70%. IR (cm⁻¹, KBr): 3400 (NH), 1681 (C=O), 1592 (C=C), 1424 (COO), 496 (Fe–Cp). Anal. Calcd for C₅₂H₄₈O₁₂N₈Fe₂Cd₂: C, 47.55; H, 3.68; N, 8.53%. Found: C, 47.17; H, 3.88; N, 8.79%. ¹H NMR (400 MHz, DMSO): δ 9.77 (m, 4H, NH), 8.35 (s, 8H, C₅H₄N), 7.62 (s, 8H, C₅H₄N), 5.07 (s, 8H, C₅H₄), 4.56 (s, 8H, C₅H₄), 1.85 (s, 12H, CH₃COO).

Crystallography. Crystal data and experimental details for compounds **1** and **2** are contained in Table 1. All measurements were made on a Rigaku RAXIS-IV imaging plate area detector with graphite monochromated Mo Kα radiation (λ = 0.710 73 Å). Red prismatic single crystals of **1** (0.30 × 0.20 × 0.20 mm³) and of **2** (0.25 × 0.20 × 0.20 mm³) were selected and mounted on a glass fiber. All data were collected at a temperature of 291(2) K

Table 1. Crystallographic Data and Structure Refinement for **1** and **2**

	1	2
formula	C ₃₂ H ₃₀ O ₉ N ₆ Fe ₂ Zn	C ₂₇ H ₂₆ O ₇ N ₄ FeHg
fw	819.69	776.96
cryst syst	monoclinic	triclinic
cryst size/mm ³	0.30 × 0.20 × 0.20	0.28 × 0.25 × 0.20
space group	P2 ₁ /c	P1
a/Å	19.280(4)	10.067(2)
b/Å	10.691(2)	10.344(2)
c/Å	17.277(4)	13.959(3)
α/deg	90	108.52(3)
β/deg	90.14(3)	99.03(3)
γ/deg	90	94.28(3)
V/Å ³	3561.3(12)	1349.1(5)
D _c /Mg m ⁻³	1.529	1.913
Z	4	2
μ/mm ⁻¹	1.532	6.275
reflns collected/unique	9881/6086	4551/4551
	R(int) = 0.0620	R(int) = 0.0000
data/restraints/params	6086/0/468	4551/0/364
R ^a	0.0615	0.0685
R _w ^b	0.1195	0.1740
GOF on F ²	1.096	1.090
Δρ _{min} and Δρ _{max} /e Å ⁻³	−0.553 and 0.471	−2.744 and 1.929

$$^a R = \sum ||F_o| - |F_c|| / \sum |F_o|. \quad ^b R_w = [\sum (|F_o| - |F_c|)^2 / \sum w|F_o|^2]^{1/2}.$$

Table 2. Selected Bond Distances (Å) and Angles (deg) for **1** and **2**

1			
Zn(1)–O(4)	1.942(4)	Zn(1)–O(3)	1.965(4)
Zn(1)–N(5)	2.025(4)	Zn(1)–N(2)	2.053(4)
C(22)–O(8)	1.218(6)	C(11)–O(7)	1.218(6)
C(11)–N(1)	1.367(7)	N(1)–C(14)	1.404(6)
C(22)–N(6)	1.387(6)	N(6)–C(19)	1.401(5)
O(4)–Zn(1)–O(3)	109.86(16)	O(4)–Zn(1)–N(2)	110.47(15)
O(4)–Zn(1)–N(5)	112.74(16)	O(3)–Zn(1)–N(2)	94.99(15)
O(3)–Zn(1)–N(5)	113.23(16)	N(5)–Zn(1)–N(2)	114.26(15)
N(4)–O(4)–Zn(1)	114.1(4)	N(3)–O(3)–Zn(1)	114.5(4)
2			
Hg(1)–O(3)	2.388(7)	Hg(1)–O(5)	2.510(7)
Hg(1)–N(1)	2.182(6)	Hg(1)–N(2)	2.173(6)
C(11)–O(1)	1.207(11)	C(22)–O(2)	1.227(10)
C(11)–N(3)	1.406(11)	C(22)–N(4)	1.373(10)
C(14)–N(3)	1.364(10)	N(4)–C(19)	1.400(9)
N(2)–Hg(1)–N(1)	163.7(3)	O(3)–Hg(1)–N(2)	94.6(3)
O(3)–Hg(1)–N(1)	90.3(3)	O(5)–Hg(1)–N(2)	99.0(2)
O(5)–Hg(1)–N(1)	95.0(3)	O(5)–Zn(1)–O(3)	103.4(2)

using the ω–2θ scan technique and corrected for Lorenz polarization effects. A correction for secondary extinction was applied.

The two structures were solved by direct methods and expanded using the Fourier technique. The non-hydrogen atoms were refined with anisotropic thermal parameters. Hydrogen atoms were included but not refined. The final cycle of full-matrix least-squares refinement was based on 6086 observed reflections and 468 variable parameters for **1** and 4551 observed reflections and 364 variable parameters for **2**. All calculations were performed using the SHELX-97 crystallographic software package.⁹ Selected bond lengths and bond angles are listed in Table 2. Additional information is available as Supporting Information. Also, these materials have been deposited with the Cambridge Crystallographic Data Center, CCDC nos. 185129 and 185131 for compounds **1** and **2**, respectively. Copies of this information can be obtained free of charge from The Director, CCDC, 12 Union Road, Cambridge CB2 1EZ, U.K. (Fax: +44.1223.336033. E-mail: deposit@ccdc.cam.ac.uk or www: http://www.ccdc.cam.ac.uk.)

(9) Sheldrick, G. M. *SHELX-97, Program for the Solution and Refinement of Crystal Structures*; University of Göttingen: Germany, 1997.

(8) Moriuchi, T.; Ikeda, I.; Hirao, T. *Organometallics* **1995**, *14*, 3578.

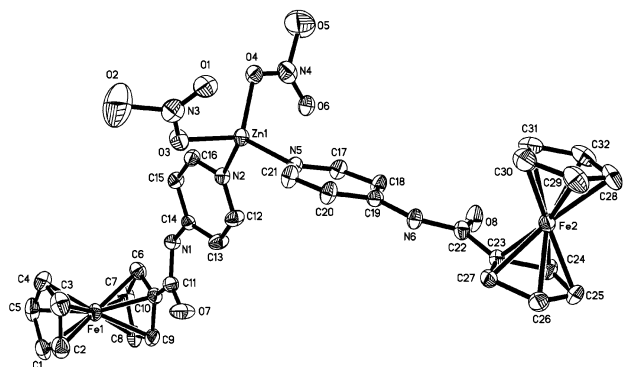


Figure 1. ORTEP drawing with atom-labeling scheme of $[\text{Zn}(\text{4-PFA})_2(\text{NO}_3)_2](\text{H}_2\text{O})$.

NLO Measurement. A DMF solution for complex 4-PFA (or 4-BPFA or **1** or **2** or **3**) was placed in a 1 mm quartz cuvette for NLO measurements. The NLO properties were determined by procedures described in previous literatures.¹⁰

Results and Discussion

Synthesis. It should be pointed out that placing the mixture of $\text{Zn}(\text{NO}_3)_2$ with 4-PFA (or $\text{Hg}(\text{OAc})_2$ or $\text{Cd}(\text{OAc})_2 \cdot 2\text{H}_2\text{O}$ with 4-BPFA) in the dark is an effective route for preparation of ferrocenyl complexes. Several groups have found that ferrocene derivatives containing an electron-withdrawing substituent on the Cp ring may provide a greater photolability and can undergo photolysis in some solvents to cause both ring-metal and ring-carbonyl cleavages.^{11,12} If the mixture of metal ions and ligand 4-PFA (or 4-BPFA) in methanol solution is under light, brown precipitate can be produced from the mixture solution. Its composition cannot be identified, so ferrocene-containing $\text{Zn}(\text{II})$ or $\text{Hg}(\text{II})$ or $\text{Cd}(\text{II})$ complexes could not be obtained. We presume that the ferrocenyl ligands undergo photolysis first and make the subsequent reactions complicated.

Crystal Structure of $[\text{Zn}(\text{4-PFA})_2(\text{NO}_3)_2](\text{H}_2\text{O})$ (1**).** The molecular structure of complex **1** was determined by single-crystal X-ray diffraction analysis. The molecule crystallizes in the space group $P2_1/c$. The perspective view together with the atomic numbering scheme is illustrated in Figure 1.

The $\text{Zn}(\text{II})$ ion is in a slightly distorted tetrahedral environment with two nitrogen atoms N2 and N5 from two 4-PFA ligands and two oxygen atoms from two nitrate anions. $\text{Zn}-\text{N}$ distances range from 2.025(4) to 2.053(4) Å, while $\text{Zn}-\text{O}$ distances are 1.942(4) and 1.965(4) Å, respectively. The $\text{Zn}-\text{N}$ distances are slightly shorter than those of other $\text{Zn}(\text{II})$ coordination polymers, for example $[\text{Zn}(\text{4,4}'\text{-bipy})(\text{H}_2\text{O})_3(\text{ClO}_4)](\text{ClO}_4) \cdot (4,4'\text{-bipy})_{1.5} \cdot \text{H}_2\text{O}$ ($\text{Zn}-\text{N}$: 2.104(2)–2.117(2) Å)^{13a} and $[\text{Zn}(\text{tp})(4,4'\text{-bipy})]$ (tp = tere-

phthalate) ($\text{Zn}-\text{N}$: 2.154(2)–2.186(3) Å),^{13b} but close to those of $\text{Zn}(\text{II})$ Schiff base complex $[\text{ZnCl}_2(\text{L}^2)]$ ($\text{L}^2 = 1,2\text{-bis}(\text{ferrocen-1-ylmethyleneamino})\text{ethane}$) ($\text{Zn}-\text{N}$: 2.063(3)–2.073(4) Å).¹⁴ Aside from the acute $\text{O}3-\text{Zn}1-\text{N}2$ angle of $94.99(15)^\circ$, other bond angles around Zn1 vary from $109.86(16)^\circ$ to $114.26(15)^\circ$. Hence, average bond angle at Zn1 is $109.25(16)^\circ$, which is close to 109.5° for an ideal tetrahedron. It is clear from the structure that one pyridyl ring is almost coplanar to the cyclopentadienyl ring plane to which it is attached; their dihedral angle (planes N5–C21 and C23–C27) is 6.5° . The dihedral angle between pyridyl ring N2–C16 and cyclopentadienyl ring C6–C10 is 19.3° . The two pyridyl rings in **1** are inclined at an angle of 72.3° .

The average $\text{Fe}-\text{C}_{\text{ring}}$ distance is 2.044(6) Å, in agreement with the value 2.04 Å of the free ferrocene. The average intra C–C bond length and C–C–C angle of cyclopentadienyl are 1.415(8) Å and $107.8(11)^\circ$, respectively, which are similar to those reported in the literature.¹⁵ The cyclopentadienyl rings are perfectly planar and nearly parallel with a dihedral angle of 0.8° at Fe1 or 1.6° at Fe2. Two planes C11–C10–O7 and C6–C10 are almost coplanar with the mean deviation from the plane being 0.0247° . Planes C22–C23–O8 and C23–C27 are also coplanar; the mean deviation from the plane is 0.0324° . The intramolecular $\text{Zn}1 \cdots \text{Fe}1$, $\text{Zn}1 \cdots \text{Fe}2$, and $\text{Fe}1 \cdots \text{Fe}2$ distances are 9.853, 9.865, and 17.807 Å, respectively. The bond distances and angles of the nitrate anion are as expected. The average N–O bond length is 1.327(6) Å, while the average intra-anion angle is $120.0(6)^\circ$.

The highly organized self-assembly is achieved in the crystal packing of **1**, wherein each molecule connects to two neighboring molecules through $\text{NH} \cdots \text{ONO}_2$ and $\text{CH} \cdots \text{ONO}_2$ bonds (Figure 2). Obviously, the $\text{NH} \cdots \text{ONO}_2$ interactions are strong. Adjacent $[\text{Zn}(\text{4-PFA})_2(\text{NO}_3)_2]$ groups are linked by intermolecular hydrogen bonds leading to an infinite chain.

Many groups have reported a large number of complexes with monosubstituted pyridine-containing ferrocene derivatives as ligands, but they focused their attention on the complexes of the middle transition metals Cr, Mo, W, Re, Os, and Rh.^{2a,k-n,5b,d,e,g} Zn complexes with monosubstituted pyridine-containing ferrocene derivatives are relatively rare.

Crystal Structure of $[\text{Hg}_2(\text{OAc})_4(\text{4-BPFA})_2](\text{CH}_3\text{OH})$ (2**).** X-ray diffraction analysis of compound **2** shows that it crystallizes in the space group $P\bar{1}$. In compound **2**, two 4-BPFA ligands bridge two $\text{Hg}(\text{II})$ ions giving a macrocycle polynuclear complex with dimensions $4.312 (\text{Hg}1 \cdots \text{Hg}1\text{A}) \times 19.589 \text{ \AA}^2 (\text{Fe}1 \cdots \text{Fe}1\text{A})$ (Figure 3). The distance between the two pyridyl rings from one 4-BPFA is ca. 3.533 Å, illustrating the intramolecular π -stacking, and the two pyridyl rings are parallel.

(10) (a) Hou, H. W.; Xin, X. Q.; Liu, J.; Chen, M. Q.; Shi, S. *J. Chem. Soc., Dalton Trans.* **1994**, 3211. (b) Sheik-Bahae, M.; Said, A. A.; Wei, T. H.; Hagan, D. J.; Van Stryland, E. W. *IEEE J. Quantum Electron.* **1990**, *26*, 760.
 (11) (a) Bergamini, P.; Di Martino, S. *J. Organomet. Chem.* **1989**, *365*, 341. (b) Ali, L. H.; Cox, A.; Kamp, T. J. *J. Chem. Soc., Dalton Trans.* **1973**, 1468. (c) Heaney, E. K.; Logan, S. R. *Inorg. Chim. Acta* **1977**, *22*, L3.
 (12) (a) Che, D. J.; Li, G.; Yao, X. L.; Zou, D. P. *J. Organomet. Chem.* **1998**, *568*, 165. (b) Che, D. J.; Li, G.; Du, B. S.; Zhang, Z.; Li, Y. H. *Inorg. Chim. Acta* **1997**, *261*, 121.

(13) (a) Tong, M. L.; Cai, J. W.; Yu, X. L.; Chen, X. M.; Ng, S. W.; Mak, T. C. W.; *Aust. J. Chem.* **1998**, *51*, 637. (b) Tao, J.; Tong, M. L.; Chen, X. M. *J. Chem. Soc., Dalton Trans.* **2000**, 3669.
 (14) Li, P.; Scowen, I. J.; Davies, J. E.; Halcrow, M. A. *J. Chem. Soc., Dalton Trans.* **1998**, 3791.
 (15) (a) Abuhijleh, A. L.; Woods, C. *J. Chem. Soc., Dalton Trans.* **1992**, 1249. (b) Takusagawa, F.; Koetzle, T. F. *Acta Crystallogr.* **1979**, *B35*, 2888. (c) Allen, T. H.; Kennard, O. *Chem. Des. Automat. News* **1993**, *8*, 146.

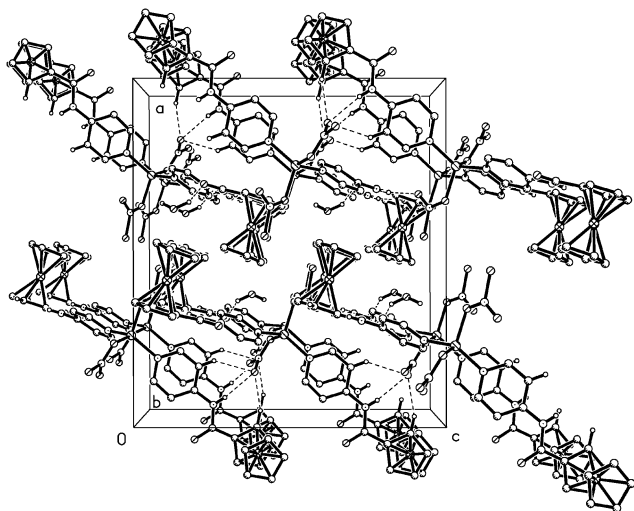


Figure 2. Crystal packing view from the *b*-axis of $[\text{Zn}(\text{4-PFA})_2(\text{NO}_3)_2] \cdot (\text{H}_2\text{O})$.

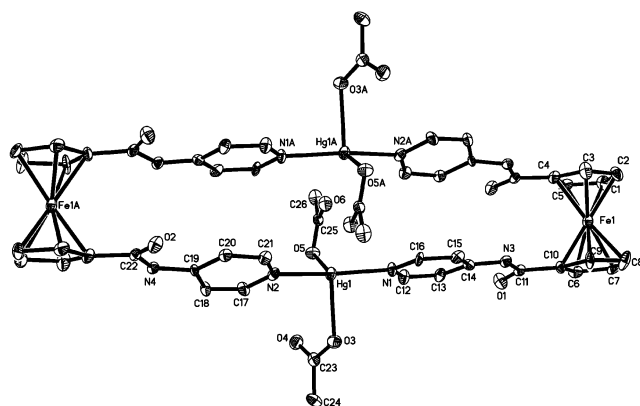


Figure 3. ORTEP drawing with atom-labeling scheme of $[\text{Hg}_2(\text{OAc})_4(\text{4-BPFA})_2](\text{CH}_3\text{OH})$ (H atoms and solvent molecule omitted for clarity).

Each Hg(II) ion is coordinated by two nitrogen atoms of two 4-BPFA ligands and two oxygen atoms of two acetate anions forming a distorted tetrahedral geometry. Hg–N bond lengths ($\text{Hg1-N1} = 2.182(6)$ Å; $\text{Hg1-N2} = 2.173(6)$ Å) are significantly shorter than those of the reported coordination polymer $\{\text{HgI}_2[\text{bpmp}]_n\}$ (bpmp = *N,N'*-bis(4-pyridylmethyl)piperazine);¹⁶ it reflects the stronger interaction between N atoms and Hg(II) ions in complex **2**. The bond lengths of Hg1–O3 and Hg1–O5 are not equal, while the average value is 2.448(7) Å. The bond angles around the Hg1 are in the range 90.3(3)–163.7(3)°, indicating a quite distorted tetrahedral geometry. The dihedral angle between pyridyl ring plane N1–C16 and cyclopentadienyl ring plane C6–C10 is 5.7°; it reveals the two ring planes are almost coplanar. However, the dihedral angle between planes N2A–C21A and C1–C5 is 18.5°, indicating a large twist.

Two cyclopentadienyl rings in each ferrocenyl fragment are planar and nearly parallel with a dihedral angle of 1.8°. Fe–C_{ring} distances ranging from 2.043(11) to 2.076(9) Å (average 2.053(11) Å) are slightly longer than those of free ferrocene, due to the interactions of the electron-withdrawing substituted group. The intracyclopentadienyl C–C bond

lengths (average 1.423(11) Å) and C–C–C angles (average 107.9(9)°) are consistent with those reported in the literature.¹⁵ The intermetallic distances of $\text{Fe1} \cdots \text{Hg1}$ and $\text{Fe1} \cdots \text{Hg1A}$ are 10.039 and 10.019 Å, respectively.

In the solid state structure of **2**, infinite $[\text{Hg}_2(\text{OAc})_4(\text{4-BPFA})_2]_n$ chains are formed by intermolecular hydrogen bonds ($\text{O} \cdots \text{H} - \text{N}$) as complex **1**. It can be seen from Figure 4 that uncoordinated O atoms (or coordinated O atoms) of acetate anions from one $[\text{Hg}_2(\text{OAc})_4(\text{4-BPFA})_2]$ group interact with NH units from neighboring $[\text{Hg}_2(\text{OAc})_4(\text{4-BPFA})_2]$ groups forming strong $\text{N} - \text{H} \cdots \text{O}$ hydrogen bonds [$\text{N3} \cdots \text{O4} = 2.897$, $\text{H3B} \cdots \text{O4} = 2.062$ Å, $\text{N3} - \text{H3B} \cdots \text{O4} = 163.52^\circ$; $\text{N4} \cdots \text{O5} = 2.929$, $\text{H4A} \cdots \text{O5} = 2.095$ Å, $\text{N4} - \text{H4A} \cdots \text{O5} = 163.27^\circ$]. Therefore, each $[\text{Hg}_2(\text{OAc})_4(\text{4-BPFA})_2]$ group joins neighboring $[\text{Hg}_2(\text{OAc})_4(\text{4-BPFA})_2]$ groups through eight $\text{N} - \text{H} \cdots \text{O}$ hydrogen bonds forming a linear chain (Figure 4). The molecular packing is shown in Figure 5. Viewed from *c*-axis, different $[\text{Hg}_2(\text{OAc})_4(\text{4-BPFA})_2]_n$ chains stack by intermolecular interactions.

Although some complexes with 1,1'-bisubstituted pyridine-containing ferrocene ligands have been described, their crystal data are limited. For instance, a list of examples follows: chain polymers $[\text{Mo}_2(\text{O}_2\text{CCF}_3)_4(\text{BPFEF})]_n$, $[\text{Rh}_2(\text{O}_2\text{CCF}_3)_4]_{n+1}(\text{BPFEF})_n$, and $[\text{Rh}_2(\text{O}_2\text{CCF}_3)_4]_n(\text{BPFEF})_{n+1}$ (BPFEF = 1,1'-bis(4-pyridylethynyl)ferrocene)^{2k} were characterized by elemental analyses, NMR, and TGA data; a trinuclear complex $[\text{MoL}^*(\text{NO})\text{Cl}_2]_2(\text{L}^3)$ ($\text{L}^* = \text{tris}(3,5\text{-dimethylpyrazolyl})\text{hydroborate}$, $\text{L}^3 = (\text{C}_5\text{H}_4\text{N})\text{CH}=\text{C}(\text{CH}_3)(\text{C}_5\text{H}_4)\text{Fe}(\text{C}_5\text{H}_4)\text{C}(\text{CH}_3)=\text{CH}(\text{C}_5\text{H}_4\text{N})$)^{2l} was verified by elemental analysis and FAB mass spectroscopy; a series of organometallic–organic hybrid crystals^{5f} from ferrocenyl dipyrindine and binaphthol were obtained; the effects of protonation on the spectroscopic and redox properties of compounds 1,1'-bis[[(6-methyl-2-pyridyl)amino]carbonyl]ferrocene and 1,1'-bis[(2-pyridylmethylamino)carbonyl]ferrocene were described by Carr et al.^{1f} Only Barranco et al.^{2d} gave the crystal structures of three complexes $[\{\text{Au}(\text{PPh}_3)\}_2\{\text{Fc}(\text{Spy})_2\}](\text{OTf})_2$, $[\{\text{Au}(\text{C}_6\text{F}_5)_3\}_2\{\text{Fc}(\text{Spy})_2\}]$, and $[\text{Ag}_2\{\text{Fc}(\text{Spy})_2\}_3](\text{OTf})_2$ ($\text{Fc}(\text{Spy})_2 = 1,1'$ -bis(2-pyridylthio)ferrocene) in 2001. To our knowledge, compound **2** is the first example of macrocyclic pyridine-containing ferrocenyl complexes.

It is to be pointed out that the IR spectra of $[\text{Cd}_2(\text{OAc})_4(\text{4-BPFA})_2]$ (**3**) are completely consistent with those of **2** in the main characteristic absorptions. This indicates that complexes **3** and **2** have a similar coordination mode. Additional support for this suggestion is given by the elemental analysis for **3**, which is in good agreement with the molecular formula.

Absorption Spectra. The UV–vis absorption spectra of ligands 4-PFA and 4-BPFA, and corresponding complexes **1–3**, were determined in a DMF solution, respectively. From previous study,^{17,18} we know that ferrocene exhibits two characteristic absorptions at 440 nm (assigned to the ${}^1\text{E}_{1g} \leftarrow {}^1\text{A}_{1g}$ transition) and 325 nm (assigned to the ${}^1\text{E}_{2g} \leftarrow {}^1\text{A}_{1g}$

(16) Niu, Y. Y.; Hou, H. W.; Wei, Y. L.; Fan, Y. T.; Zhu, Y.; Du, C. X.; Xin, X. Q. *Inorg. Chem. Commun.* **2001**, *4*, 358.

(17) Sohn, Y. S.; Hendrickson, D. N.; Gray, H. B. *J. Am. Chem. Soc.* **1971**, *93*, 3603.

(18) Armstrong, A. T.; Smith, A. T.; Elder, E.; McGlynn, S. P. *J. Chem. Phys.* **1967**, *46*, 4321.

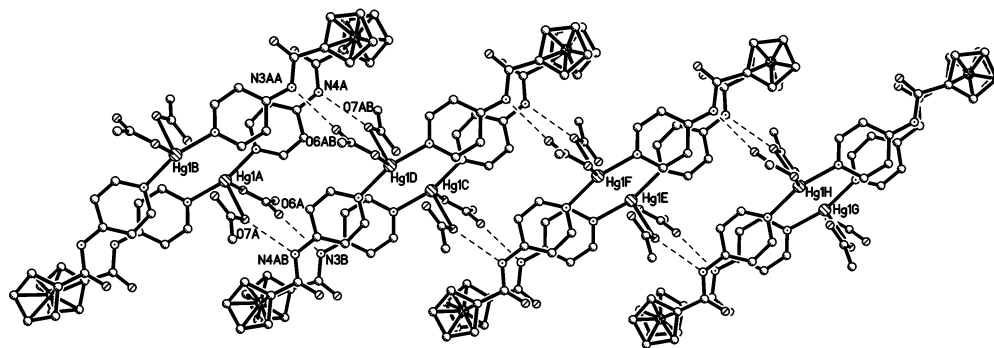


Figure 4. One-dimensional chain supported by hydrogen bonding of $[\text{Hg}_2(\text{OAc})_4(4\text{-BPFA})_2](\text{CH}_3\text{OH})$.

transition). 4-PFA and $[\text{Zn}(4\text{-PFA})_2(\text{NO}_3)_2](\text{H}_2\text{O})$ (**1**) give very similar absorption spectra; the two absorptive peaks at 321 and 431 nm indicate a slight blue-shift compared to those of free ferrocene. Similarly, ligand 4-BPFA and complexes $[\text{Hg}_2(\text{OAc})_4(4\text{-BPFA})_2](\text{CH}_3\text{OH})$ (**2**) and $[\text{Cd}_2(\text{OAc})_4(4\text{-BPFA})_2]$ (**3**) show two characteristic bands, too; the effective bands around 270 nm may be attributed to the metal–ligand charge transfer (MLCT) transitions. All the five compounds have relatively low linear absorption ranging from 450 to 1000 nm, promising low intensity loss and little temperature change caused by photon absorption when light propagates in the materials.

NLO Properties. The Z-scan measurements were carried out with a 532 nm laser pulse of 8 ns duration in a DMF solution of $3.27 \times 10^{-4} \text{ mol dm}^{-3}$ for 4-PFA, $2.35 \times 10^{-4} \text{ mol dm}^{-3}$ for 4-BPFA, $1.22 \times 10^{-4} \text{ mol dm}^{-3}$ for **1**, $6.45 \times 10^{-5} \text{ mol dm}^{-3}$ for **2**, or $7.65 \times 10^{-5} \text{ mol dm}^{-3}$ for **3**.

The NLO refractive effects were assessed by dividing the normalized Z-scan data obtained under closed-aperture configuration by the normalized Z-scan data obtained under the open-aperture configuration. An effective third-order NLO refractive index n_2 can be derived by eq 1:

$$n_2 = \frac{\lambda \alpha_0}{0.812\pi I(1 - e^{-\alpha_0 L})} \Delta T_{V-P} \quad (1)$$

where ΔT_{V-P} is the difference between normalized transmittance values at valley and peak portion. I is the peak irradiation intensity at focus ($4.2 \times 10^{12} \text{ W/m}^2$), α_0 is the linear absorption coefficient, L is the sample thickness (1 mm in this study), and λ is the wavelength of the laser (532 nm). Figure 6 shows the NLO refractive effects of ligands 4-PFA and 4-BPFA and complexes **1–3**. The ΔT_{V-P} and α_0 values of these compounds are listed in Table 3. The data show that these compounds have a similar positive sign for the refractive nonlinearity, which gives rise to self-focusing behavior. The calculated refractive index n_2 values are shown in Table 3. The values are in the range 1.53×10^{-17} to $3.67 \times 10^{-17} \text{ m}^2 \text{ W}^{-1}$. Similar refractive effects can be found in some reported clusters $\text{MoCu}_2\text{OS}_3(\text{PPh}_3)_3$ ($n_2 = 5.0 \times 10^{-17} \text{ m}^2 \text{ W}^{-1}$), $\text{WCu}_2\text{OS}_3(\text{PPh}_3)_4$ ($n_2 = 8.0 \times 10^{-18} \text{ m}^2 \text{ W}^{-1}$), and $\text{W}_2\text{Ag}_4\text{S}_8(\text{AsPh}_3)_4$ ($n_2 = 5.9 \times 10^{-17} \text{ m}^2 \text{ W}^{-1}$).^{19,20}

(19) Shi, S.; Hou, H. W.; Xin, X. Q. *J. Phys. Chem.* **1995**, *99*, 4050.

(20) Sakane, G.; Shibahare, T.; Hou, H. W.; Xin, X. Q.; Shi, S. *Inorg. Chem.* **1995**, *34*, 4785.

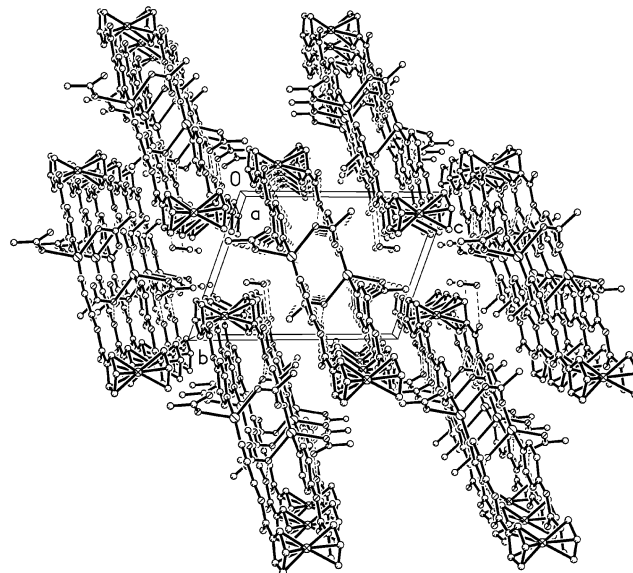


Figure 5. Crystal packing view from the a -axis of $[\text{Hg}_2(\text{OAc})_4(4\text{-BPFA})_2](\text{CH}_3\text{OH})$.

In accordance with the n_2 values, the effective third-order NLO susceptibility $\chi^{(3)}$ values can be calculated by $\chi^{(3)} = cn_0^2 n_2 / 80\pi$, where c is speed of light in a vacuum and n_0 is the linear refractive index of the sample (~ 1.43). The $\chi^{(3)}$ values are also listed in Table 3. The corresponding modulus of the hyperpolarizability γ values were obtained from $|\gamma| = \chi^{(3)} / NF^4$, where N is the number density of a ferrocenyl compound in the sample (in cm^{-3}) ($N = 10^{-3} \times CN_A$, C is the molar concentration of the compound in a DMF solution, N_A is the Avogadro constant); $F^4 = 3$ is the local field correction factor. The calculated γ values for compounds 4-PFA, **1**, 4-BPFA, **2**, and **3** are 1.51×10^{-28} , 2.46×10^{-28} , 1.53×10^{-28} , 3.12×10^{-28} , and 3.10×10^{-28} esu, respectively (Table 3). The γ values are nearly twice as large for complexes **1–3** as for their individual ligands. A reasonable explanation is that post-transition metals Zn, Cd, or Hg have no influence on the strength of NLO properties; in Zn, Cd, or Hg, there is no an open d-shell, they lack low energy charge transfer transitions, and thus, their contribution to optical nonlinearity can be ignored. We notice that **2** and **3** have the same γ values regardless of Cd and Hg. The γ values of complexes **1–3** are dominated by 4-PFA or 4-BPFA; there are two 4-PFA ligands in compound **1** and two 4-BPFA ligands in compound **2** or **3**, so the γ values for the complexes **2** (3.12×10^{-28} esu) and **3** (3.10×10^{-28}

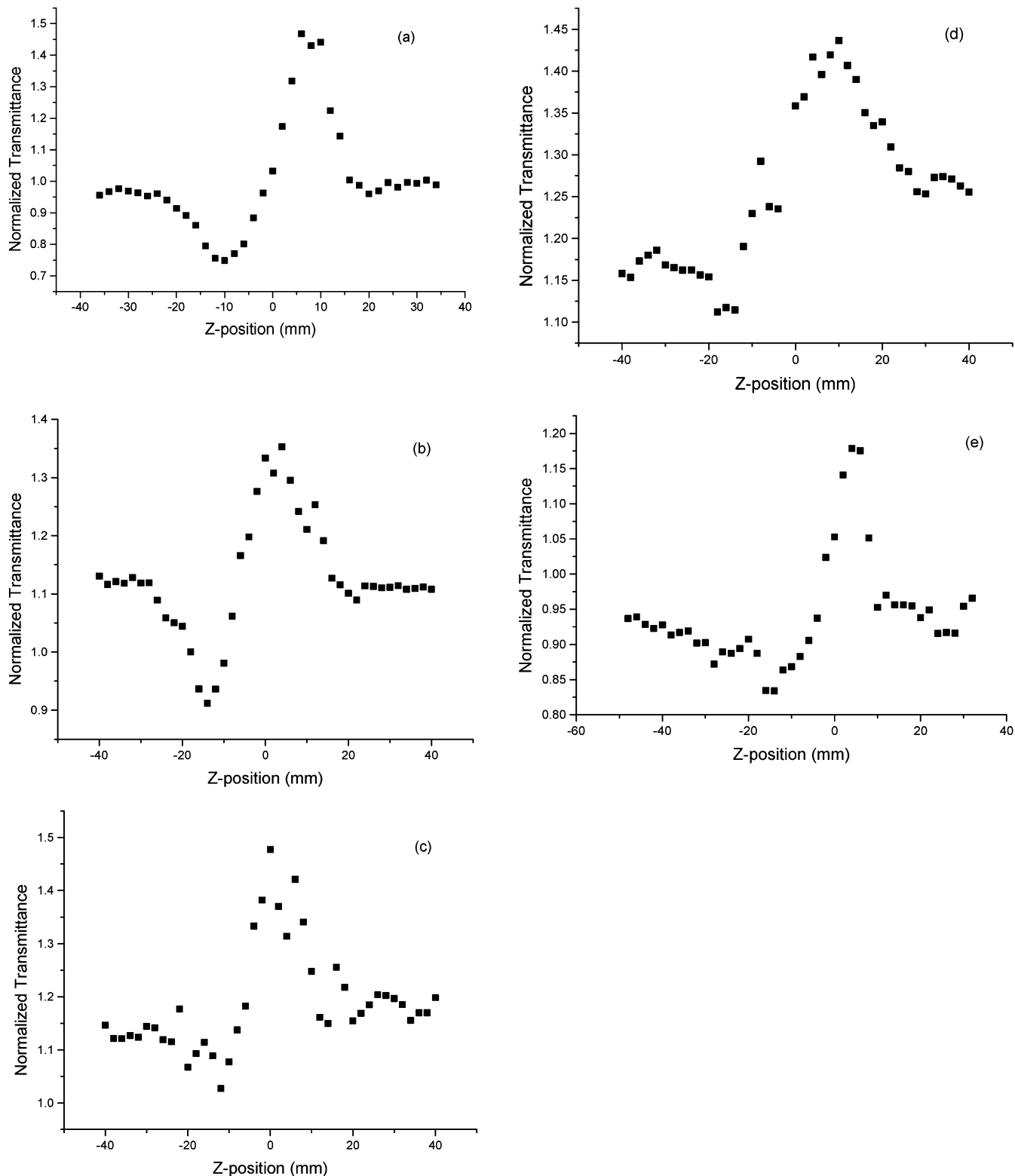


Figure 6. Data were assessed by dividing the normalized Z-scan data obtained under the closed-aperture configuration by the normalized Z-scan data obtained under the open-aperture configuration. (a) The self-focusing effects of 4-PFA in $3.27 \times 10^{-4} \text{ mol}\cdot\text{dm}^{-3}$ DMF solution at 532 nm. (b) The self-focusing effects of $[\text{Zn}(\text{4-PFA})_2(\text{NO}_3)_2](\text{H}_2\text{O})$ (**1**) in $1.22 \times 10^{-4} \text{ mol}\cdot\text{dm}^{-3}$ DMF solution at 532 nm. (c) The self-focusing effects of 4-BPFA in $2.35 \times 10^{-4} \text{ mol}\cdot\text{dm}^{-3}$ DMF solution at 532 nm. (d) The self-focusing effects of $[\text{Hg}_2(\text{OAc})_4(\text{4-BPFA})_2](\text{CH}_3\text{OH})$ (**2**) in $6.45 \times 10^{-5} \text{ mol}\cdot\text{dm}^{-3}$ DMF solution at 532 nm. (e) The self-focusing effects of $[\text{Cd}_2(\text{OAc})_4(\text{4-BPFA})_2]$ (**3**) in $7.65 \times 10^{-5} \text{ mol}\cdot\text{dm}^{-3}$ DMF solution at 532 nm.

esu) are twice as large as those for the corresponding ligand 4-BPFA (1.53×10^{-28} esu). For compound **1**, the γ value (2.46×10^{-28} esu) is a bit less than twice the value for the ligand 4-PFA (1.51×10^{-28} esu) considering the experi-

mental errors in the data. The conclusion can be confirmed by Tian et al.'s result.²⁵ The γ values of complexes NiL_4^2 (2.70×10^{-33} esu) and PdL_4^2 (3.06×10^{-33} esu) are 2 orders of magnitude larger than those of the ligand $\text{FcC}(\text{CH}_3)=\text{N}_2-$

Table 3. Measurement Results of a Series of Ferrocenyl Organometallics Using Z-scan Techniques

compounds	$C/\text{mol dm}^{-3}$	ΔT_{V-P}	α_0/cm^{-1}	$n_2/\text{m}^2\text{W}^{-1}$	$\chi^{(3)}/\text{esu}$	γ/esu
4-PFA	3.27×10^{-4}	0.740	1.31	3.67×10^{-17}	8.97×10^{-11}	1.51×10^{-28}
1	1.22×10^{-4}	0.446	1.60	2.22×10^{-17}	5.43×10^{-11}	2.46×10^{-28}
4-BPFA	2.35×10^{-4}	0.447	0.82	2.67×10^{-17}	6.51×10^{-11}	1.53×10^{-28}
2	6.45×10^{-5}	0.329	2.85	1.53×10^{-17}	3.72×10^{-11}	3.12×10^{-28}
3	7.65×10^{-5}	0.347	1.07	1.72×10^{-17}	4.20×10^{-11}	3.10×10^{-28}

Table 4. Optical Parameters of Selected NLO Chromophores

compounds	γ/esu	λ/nm	pulse width	ref
Cluster Compounds				
$\text{MoCu}_2\text{OS}_3(\text{PPh}_3)_3^a$	9.8×10^{-28}	532	7 ns	19
$\text{WCu}_2\text{OS}_3(\text{PPh}_3)_4^a$	9.0×10^{-29}	532	7 ns	19
$\text{W}_2\text{Ag}_4\text{S}_8(\text{AsPh}_3)_4^a$	8.3×10^{-28}	532	7 ns	20
$[\text{WOS}_3\text{Cu}_3(\text{SCN})(\text{Py})_5]^a$	2.2×10^{-27}	532	7 ns	21
$[\text{MoOS}_3\text{Cu}_3(\text{SCN})(\text{Py})_5]^a$	5.8×10^{-27}	532	7 ns	21
$\{[\text{Et}_4\text{N}]_2[\text{MoS}_4\text{Cu}_4(\text{CN})_4]\}_n^a$	1.2×10^{-29}	532	7 ns	22
$\{[\text{Et}_4\text{N}]_2[\text{WS}_4\text{Cu}_4(\text{CN})_4]\}_n^a$	1.3×10^{-29}	532	7 ns	22
$[\text{Et}_4\text{N}]_3[\text{WOS}_3(\text{CuBr})_3(\mu_2\text{-Br})] \cdot 2\text{H}_2\text{O}^a$	1.6×10^{-28}	532	7 ns	23
$[\text{Et}_4\text{N}]_3[\text{WOS}_3(\text{CuI})_3(\mu_2\text{-I})]^a$	2.8×10^{-29}	532	7 ns	24
Ferrocenyl Complexes				
$\text{FcC}(\text{CH}_3)=\text{N}_2\text{HCS}_2\text{CH}_2\text{C}_6\text{H}_5 (\text{L}^4)^b$	3.11×10^{-35}	308	16 ns	25
NiL^4_b	2.71×10^{-33}	308	16 ns	25
PdL^4_b	3.06×10^{-33}	308	16 ns	25
ferrocene ^b	$1.61 \pm 0.18 \times 10^{-35}$	602	400 fs	26
ferrocenecarboxaldehyde ^b	$1.69 \pm 0.08 \times 10^{-35}$	602	400 fs	26
$\text{FcCH}=\text{CHC}_6\text{H}_5^b$	$8.55 \pm 1.98 \times 10^{-35}$	602	400 fs	26
$1,1'\text{-Fc}(\text{CH}=\text{CHC}_6\text{H}_5)_2^b$	$2.70 \pm 0.26 \times 10^{-34}$	602	400 fs	26
$\text{CHO}(-\text{FcCH}=\text{CHC}_6\text{H}_5\text{CH}=\text{CH}-)_n^b$	$1.55 \pm 0.27 \times 10^{-33}$	602	400 fs	26
1,8-bis(ferrocenyl)octatetrayne ^c	1.10×10^{-34}	19.1	10ns	27
4-PFA ^a	1.51×10^{-28}	532	7 ns	this work
1 ^a	2.46×10^{-28}	532	7 ns	this work
4-BPFA ^a	1.53×10^{-28}	532	7 ns	this work
2 ^a	3.12×10^{-28}	532	7 ns	this work
3 ^a	3.10×10^{-28}	532	7 ns	this work

^a Z-scan technique. ^b Degenerate four-wave mixing technique (DFWM). ^c DC electric field induced second-harmonic generation technique (EFISH).

$\text{HCS}_2\text{CH}_2\text{C}_6\text{H}_5 (\text{L}^4)$ (3.11×10^{-35} esu).²⁵ This is mainly due to the existence of transition metal ions Ni(II) and Pd(II). Unlike Zn, Cd, and Hg, Ni and Pd have an open d-shell involving the low energy charge transfer transitions, which can give an important contribution to optical nonlinearity. From these discussions, we can reasonable state that transition metals (such as Ni and Pd) in ferrocenyl complexes can give a larger contribution to optical nonlinearity than that of the ferrocenyl ligands, but the influence of post-transition metals (Zn, Cd, or Hg) to optical nonlinearity is small.

The γ values of some ferrocene derivatives obtained by different methods have been reported. For example, Ghosal et al.²⁶ have reported the γ values of aryl and vinyl derivatives of ferrocene ranging from $1.61 \pm 0.18 \times 10^{-35}$ to $1.550 \pm 0.270 \times 10^{-33}$ esu. Yuan et al.²⁷ have described

the γ value for 1,8-bis(ferrocenyl)octatetrayne being 1.10×10^{-34} esu. It has been reported that the γ values of aryl and vinyl of ferrocene strongly increase with the length of the conjugated π -electron system.²⁶ Obviously, the conjugation of the pyridine and the ferrocene groups in the title ferrocenyl compounds may give some influence on optical nonlinearity. It can be seen from Table 4 that the γ values of 4-PFA, 4-BPFA, **1**, **2**, and **3** are close to those of reported clusters (the NLO properties of these compounds were measured under the same conditions).^{19–24} From this point of view, the title compounds are promising candidates for third-order NLO materials.

To the best of our knowledge, there are no reports about third-order NLO properties of these types of ferrocenyl organometallics. We believe that our explorations may provide a useful guide to the design of third-order NLO materials.

Acknowledgment. The authors thank the National Natural Science Foundation of China, Outstanding Young Teacher Foundation of Ministry of Education of China, and Innovation Foundation of Henan Province for financial supported.

Supporting Information Available: Crystallographic data in CIF and pdf formats. This material is available free of charge via the Internet at <http://pubs.acs.org>.

IC0258633

- (21) Hou, H. W.; Ang, H. G.; Ang, S. G.; Fan, Y. T.; Low, M. K. M.; Ji, W.; Lee, Y. W. *Phys. Chem. Chem. Phys.* **1999**, *1*, 3145.
 (22) Zhang, C.; Song, Y. L.; Xu, Y.; Fun, H. K.; Fang, G. Y.; Wang, Y. X.; Xin, X. Q. *J. Chem. Soc., Dalton Trans.* **2000**, 2823.
 (23) Chen, Z. R.; Hou, H. W.; Xin, X. Q.; Yu, K. B.; She, S. *J. Phys. Chem.* **1995**, *99*, 8717.
 (24) Hou, H. W.; Liang, B.; Xin, X. Q.; Yu, K. B.; Ge, P.; Ji, W.; Shi, S. *J. Chem. Soc., Faraday Trans.* **1996**, *92*, 2343.
 (25) Tian, Y. P.; Lu, Z. L.; You, X. Z. *Acta Chim. Sin. (Chin. Ed.)* **1999**, *57*, 1068.
 (26) Ghosal, S.; Samoc, M.; Prasad, P. N.; Tufariello, J. J. *J. Phys. Chem.* **1990**, *94*, 2847.
 (27) Yuan, Z.; Stringer, G.; Jobe, I. R.; Kreller, D.; Scott, K.; Koch, L.; Taylor, N. J.; Marder, T. B. *J. Organomet. Chem.* **1993**, *452*, 115.